Organic light-emitting diodes

21

Paul-Anton Will, Sebastian Reineke
Dresden Integrated Center for Applied Physics and Photonic Materials (IAPP) and Institute of Applied Physics, Technische Universität Dresden, Dresden, Germany

21.1 Introduction

Organic light-emitting diodes (OLEDs) are solid-state light sources made of organic semiconductor (OSC) materials. Various functional materials help to facilitate the conversion of injected charges into emitted photons at the maximum possible efficiency and further are assembled specifically to realize the desired emitted color—be it monochrome or broadband emissions for displays or solid-state lighting (SSL), respectively. The materials used can be both small molecules (Tang and VanSlyke, 1987) and polymers (Burroughes et al., 1990), where any possible combination of the two material classes best meets the requirements with respect to desired applications and most suitable processability. With few exceptions, the organic materials can be made and upscaled at low cost, and their processing schemes suggest truly economic mass production. For the first applications entering the market (i.e., small displays for handheld devices like smart phones and tablets), the production of such panels is already profitable. For any possible application, the effort to create even better devices has not come to an end, where efficiency, cost of production, and long-term stability are the key drivers for research and development. For OLEDs, the virtually unlimited pool of possible materials (Reymond et al., 2011) amounts to boon and bane at once. While the toolbox of organic synthesis allows subtle material adjustments and optimizations, it turns research and development into a multidimensional problem. This reduces the pace of progress and is heavy on resources, and therefore machine-learning techniques (Gómez-Bombarelli et al., 2016) have begun to be used to cope with this grand material space. On top of this, the material development cannot fully be decoupled from their processing, which is why it is still not clear which processing technology (vacuum deposition or printing) ultimately will find broad utilization.

This chapter will present an introduction to OLEDs and discuss their device- and application-specific technological aspects. For the purpose of this introduction, first-hand device designs and data of selected OLEDs from the authors will be used to support the arguments and offer a coherent discussion. These results displayed here are based on small-molecule, vacuum-processed devices. Again, within the boundaries of material processability and compatibility, these concepts and phenomena can be transferred to any given system, including all-polymer devices.

Handbook of Organic Materials for Electronic and Photonic Devices. https://doi.org/10.1016/B978-0-08-102284-9.00021-8

21.2 Fundamentals of OLEDs

21.2.1 Architecture and working principle

OLEDs are thin-film devices consisting of a carefully optimized sequence of OSCs, where each material fulfills a certain function, which will be defined next. These layers are sandwiched between electrodes to allow charge-carrier injection as a result of externally applied bias. Fig. 21.1A shows a schematic cross section of an OLED. Here, holes and electrons are injected from an anode and a cathode, respectively, where their recombination in the center of the layers ultimately generates photons that give rise to electroluminescence (EL). Compared to inorganic materials, OSCs have low charge-carrier mobility (typical values in the range of 10^{-8}–10^{-2} $cm^2/(Vs)$),

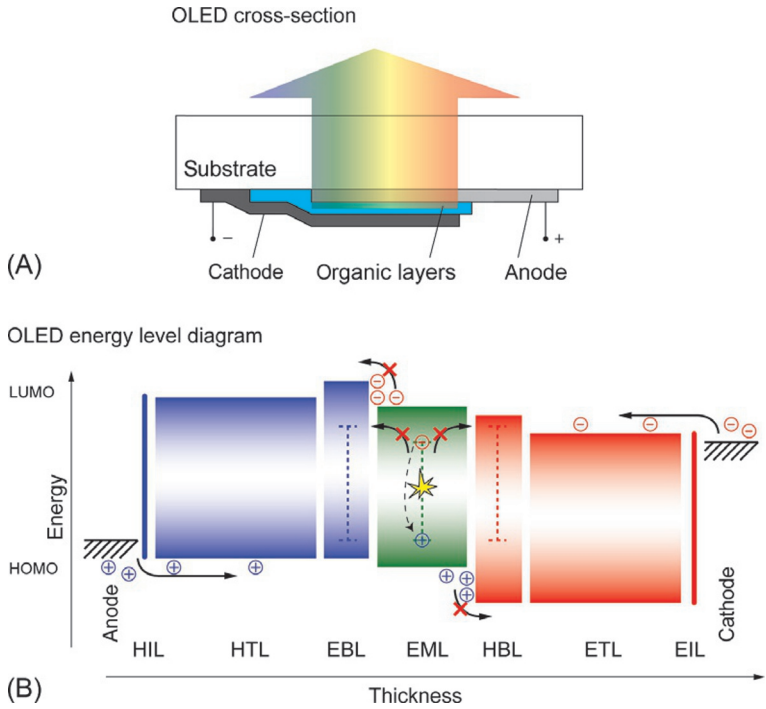

Fig. 21.1 General illustration of an OLED. (A) Cross-section schematic of an OLED, indicating the sandwich structure of electrodes and the OSC materials and the transparent substrate. Anode and cathode, which sandwich the organic functional layers, define the lateral active area by their mutual overlap. (B) Energy-level diagram of a multilayer OLED. From anode to cathode, the functional layers are: hole injection layer (HIL), hole transport layer (HTL), electron blocking layer (EBL), emission layer (EML), hole blocking layer (HBL), electron transport layer (ETL), and electron injection layer (EIL). The recombination takes place in the EML. Dashed lines indicate the triplet energy levels of the EBL, EML, and HBL. Here, energy transfer losses from EML to the blocking layers should be suppressed.
Source: SR/IAPP.

which dictates the limits for the vertical device dimension. Here, the overall thickness of an OLED typically ranges from 100 to 200 nm, only accounting for organic materials. Thicker devices are not feasible simply because the limited transport properties of OSCs would introduce significant resistive losses. Here, only the introduction of *p*- and *n*-doped transport layers (Walzer et al., 2007) alleviates this limitation, and consequently, thicker devices are possible. The fabrication methods that can be used for these organic materials (Forrest, 2004) allow for laterally scaling the dimensions of this fundamental design so that OLEDs are a true area light source.

Fig. 21.1B shows an energy-level diagram of a multilayer OLED, where the typical position of the electrode work functions and the OSC highest occupied and lowest unoccupied molecular orbitals (HOMOs and LUMOs, respectively) are indicated. The application of an external electric field leads to carrier injection from the contacts. Here, drift and diffusion determine the overall flow and distribution of the charge carriers. The devices are designed in a way that allows for effective and barrier-free transport of the two carrier types from the electrodes to the most central layer (i.e., the emission layer (EML)). Most of the distance, designated carrier transport layers (hole transport layer (HTL) and electron transport layer (ETL), respectively) support the transport of charges. These layers are usually the thickest of the organic layers, as they also serve as an optical spacer to maximize light outcoupling. To allow efficient recombination of these free and uncorrelated charge carriers to states that mediate the conversion to photons—the so-called excitons, which can be seen as Coulomb-bound electron-hole pairs—the energy level of the subsequent layer after the EML with respect to the injecting electrode is chosen to have a large energy barrier. These layers are called electron and hole blocking layers (EBL and HBL, respectively). In addition to keeping charge carriers confined to the EML, these layers need to allow for excitonic confinement (Goushi et al., 2004), especially in the case of long-lived triplet excitons (cf. Section 21.3.2); and finally, they need to decouple the HTL and ETL from the EML, whenever those comprise conductive dopants. Otherwise, such dopants would increase excitonic losses, as they often represent effective quenching sites. The injection from the electrodes into the respective transport layers can be made efficient by one of the following three approaches: (1) energetic matching of the electrode work function to the HOMO/LUMO of the OSC material (Koch, 2007); (2) electrical doping of the transport layers, which leads to significant band bending and, consequently, efficient tunnel injection through a formed depletion layer (Walzer et al., 2007; Olthof et al., 2009); or (3) the use of injection layers, which modify the energetics of the interface significantly, which in the most extreme case leads to ohmic injection (Greiner et al., 2012; Kotadiya et al., 2018). While the latter two approaches allow for comparably free choice of the respective electrode materials as they tolerate energy mismatch to a certain extent, the former needs a cautious optimization of the electrode/OSC interfaces.

The historic and most common OLED design comprises a transparent anode (indium tin oxide—ITO) on a transparent carrier substrate, an organic multilayer stack of functional molecules, and ultimately a highly reflective metal cathode (cf. Fig. 21.1A). This allows efficient light outcoupling of direct and reflected parts of the internally generated photon flux and is referred to as *bottom-emitting OLED*.

The optics of OLEDs is far more complex, but still, the required application scenario will always define the general device layout, as discussed further in Section 21.3.3. As the layers including electrodes can be fabricated in virtually any sequence, many different layouts have become popular: (1) top-emitting OLEDs, where the function of transparent and reflective electrodes are switched to allow efficient emission to take place away from the substrate; (2) transparent OLEDs with two transparent electrodes to generate emission in both directions; (3) inverted OLEDs, having the organic layers flipped so that the first electrode becomes the electron-injecting one; and (4) stacked OLEDs, where similar or different full OLED multilayers are stacked vertically. The last design is very attractive for both color mixing and improvements of device lifetime on industrial levels.

21.2.2 Monochrome OLEDs

Monochrome OLEDs are devices where EL originates from one type of emitter molecule. These type of OLEDs are the basis for the display technology, as their red, green, blue (RGB) versions (Meerheim et al., 2008; Adachi et al., 2001a,b; Lee et al., 2016) form the primary colors to span the desired color space (cf. Fig. 21.2). This is why OLEDs with dedicated color close to the display specifications (e.g., the NTSC standard) are investigated and developed with a particularly high interest, despite the fact that all other colors (e.g., yellow or sky-blue (a color between blue and green)) are possible with the right emitter at hand (Liu et al., 2017; Lee et al., 2012; Fan et al., 2013).

Fig. 21.2 shows representative current density-voltage-luminance (*j-V-L*) characteristics and the EL spectra for three representative emitters. Also shown are the chemical structures of the three emitters. In the *j-V* data, the exponential regime, visible here as a sudden increase of the current density above $V > 2\,\mathrm{V}$ exceeding the leakage current regime, scales with the band gap of the emitters used. For this point in the *j-V* characteristics, often the term *turn-on voltage* is used (Tanaka et al., 2007; Su et al., 2008), and it is correlated to the peak emission wavelength of the EL. Even more reports suggest that EL takes place at or even below the theoretical limit (i.e., when $E_{\mathrm{peak}} \geq eV_{\mathrm{on}}$). However, there are two points to consider: First, the value of V_{on} cannot be determined experimentally properly, as it depends on a parasitic level of the leakage current; and second, emission at voltages below the peak energy E_{peak} is possible and can be explained with established semiconductor theory (Würfel, 2005). Apart from the expected correlation of the onset of the exponential regime of the three example OLEDs with the emitter band gap, the overall shape of the curves differs. As the *j-V* characteristics are a consequence of bipolar transport through various layers and across various interfaces and recombination to neutral excitons, many material- and architecture-related parameters influence the overall transport of charge carriers. Here, sophisticated drift diffusion (Schober et al., 2010) or kinetic Monte-Carlo (Coehoorn et al., 2015; Mesta et al., 2013) simulations are needed to explain the experimental data.

The EL in Fig. 21.2B shows typical spectral distributions—one for a blue fluorescent emitter and two for phosphorescent green and red emitters. While all these

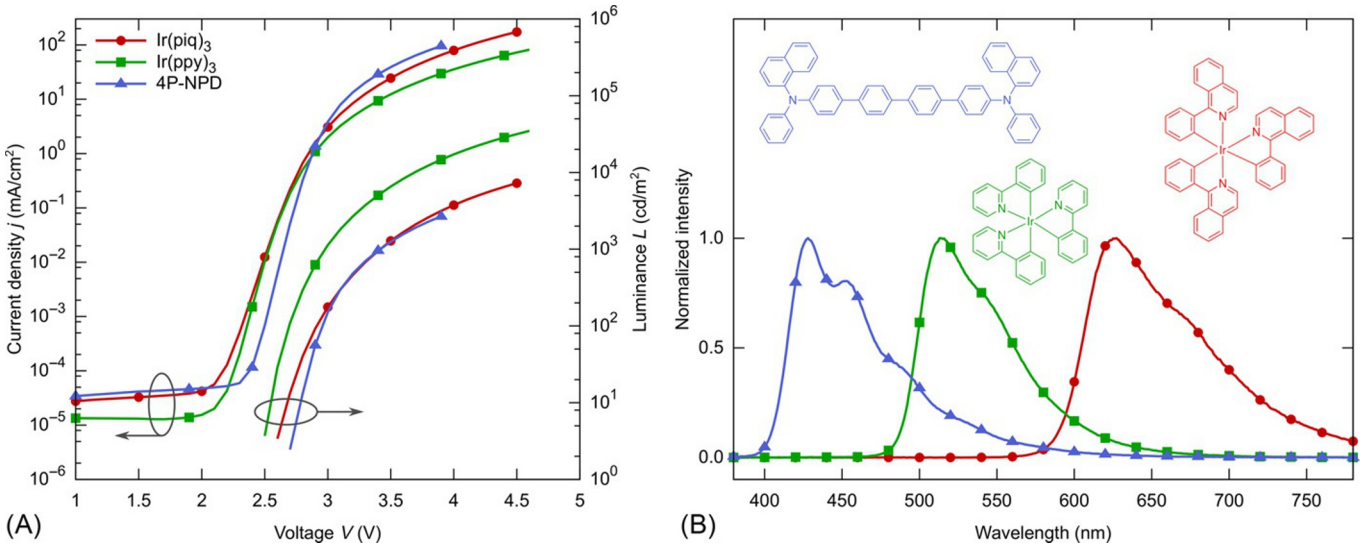

Fig. 21.2 Key device characteristics of three representative monochrome OLEDs (*red*, *green*, and *blue*). (A) Current density-voltage-luminance (*j-V-L*) characteristics. (B) Chemical structures of the emitter molecules and EL spectra of the same devices.
Credit: PAW/IAPP.

single-emitter devices are referred to as *monochrome OLEDs,* as mentioned previously, their spectrum strongly differs from a purely monochrome color stimulus. Typical full width at half maximum (FWHM) values are in the range of 50–100 nm (Reineke et al., 2010). For display applications, the FWHM of the EL spectrum is subject to optimization, where smaller values improve color purity, which is especially important for green emitters, as they can comprise blue and red parts of the spectrum. The narrowing of the FWHM can be achieved through the design of either the emitter molecules (Fleetham et al., 2014; Li et al., 2014) or the optical device (Meerheim et al., 2008).

It is important to note that there are two distinct concepts for realizing the EML of a monochrome device. Either a host-guest system or a bulk emitter film is used. In the former, the guest is the emitter molecule and the host an energetically suited wide-band-gap material embedding the emitter. The host material is often needed because many emitters do not show efficient luminescence at high concentrations due to emitter aggregation (Kawamura et al., 2006). To prevent this aggregation effect, the emitter is diluted into the host material. This concept also can serve the purpose to decouple the emitter from transport duties, which may prove beneficial for both the efficiency and stability of the OLEDs. Alternatively, monochrome OLEDs can be made from bulk films of emitters (Rosenow et al., 2010). This is possible whenever the emitter behaves different to the trend mentioned here (i.e., it shows efficient luminescence at high concentration—an effect called *aggregation-induced emission (AIE)*). These arguments hold equally true for the development of white OLEDs.

21.2.3 White light-emitting OLEDs

White OLEDs were initially developed for their potential use in general lighting settings, but are currently mostly used in large-panel displays in the red, green, blue, white (RGBW) concept discussed in Section 21.4.1, where white EL is used as the primary color and converted into differently emitting pixels in combination with color filters. In general, white light can be realized even with a set of different monochromatic spectral lines distributed in the color space. At the same time, the color perception of objects illuminated by such a white light source—quantified by the so-called color-rendering index (CRI; Reineke et al., 2013)—would be poor. Here, the spectral broadness of organic emitters (FWHM typically between 50 and 100 nm) used in OLEDs are advantageous (Reineke et al., 2010). Fig. 21.3 shows the primary EL spectra of the RGB emitters $Ir(piq)_3$, $Ir(ppy)_3$, and 4P-NPD, respectively. Their spectra mark certain positions in the CIE color space, as shown in the center graph in the figure. The emitter contributions can be mixed in an additive fashion to generate white light. To realize high CRI values, the generated EL should be designed to match the emitted spectrum of a given black-body radiator with the corresponding color temperature on the Planckian locus (Jou et al., 2013; Wu et al., 2016). There are two important color points on the Planckian locus: points E and A, which are widely accepted color standards. Point E is often referred to as the *point of equal energy,* which qualitatively fits with the very similar contributions of the composing monochrome emission bands (cf. Fig. 21.3). In contrast, point A, the *warm white color point*, contains

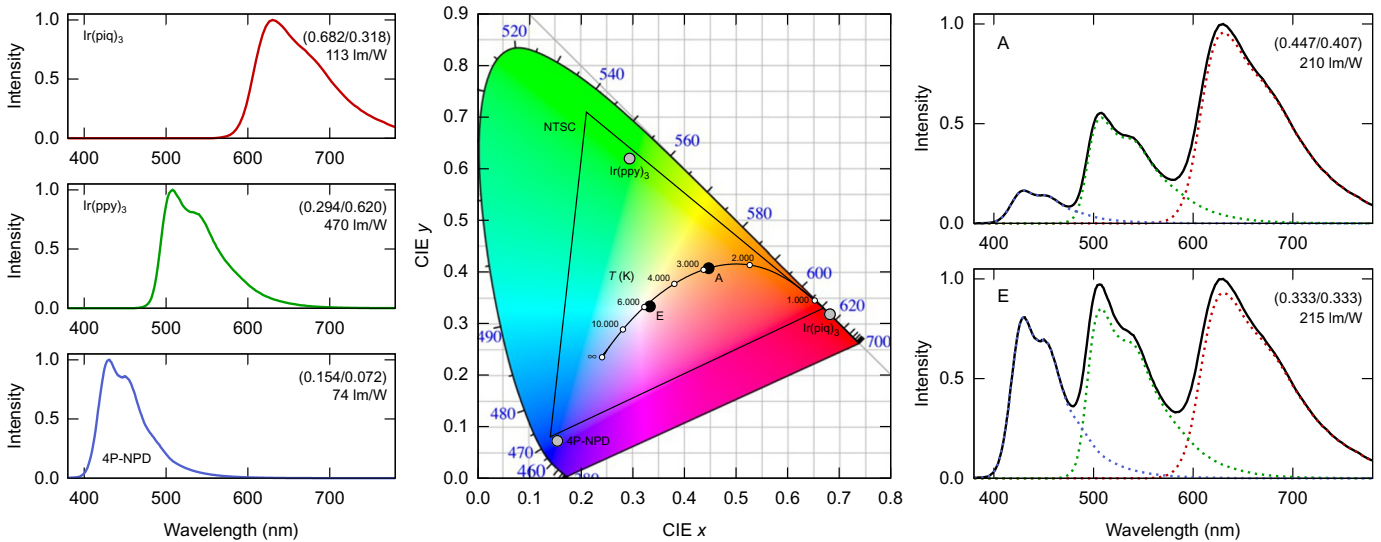

Fig. 21.3 The CIE 1931 color space (center) and various representative EL spectra generated by OLEDs. The spectra of the monochrome OLEDs (left) are experimental data based on the emitters $Ir(piq)_3$ *(red)*, $Ir(ppy)_3$ *(green)*, and 4P-NPD *(blue)*. Their associated color points are labeled in the CIE 1931 diagram. The shown white spectra (right) are calculated based on different compositions of these primary monochrome devices to demonstrate white spectra at color points A and E. Also shown here are the NTSC display standard *(black triangle)* and the Planckian locus (*black curve*; the different values represent perceived colors of a black body radiator at various temperatures). The values in each spectral plot are CIE (*x*/*y*) coordinates and the luminous efficacy of radiation K_r.
Source: PAW/IAPP.

much less blue light. The value K_r given in the panels of Fig. 21.3 for the various spectra is called *luminous efficacy of radiation*, and it represents a conversion of radiometric and photometric units. Its value is directly proportional to the luminous efficacy (given in lumens per watt) of the final device, which is the figure of merit for light sources. For instance, comparing the values $K_{r,\,E} = 215\,\text{lm/W}$ and $K_{r,\,A} = 210\,\text{lm/W}$ for the abovementioned color points and the very spectra shown in Fig. 21.3, one can directly derive that intrinsically the spectrum at color point E will yield slightly higher luminous efficacy values. The CRI values of the two white spectra are 69 and 61 for color points E and A, respectively. Clearly, these values are not very high, which is due to the significant gaps between the individual emission bands.

Technologically, there are many ways to realize white EL from OLEDs (Reineke et al., 2013). Fig. 21.4 summarizes various white OLED designs. White light emission can be realized by an assembly of monochrome OLEDs, which can be fabricated either in a vertical (Bulovic et al., 1996; Rosenow et al., 2010) or horizontal (Krotkus et al., 2016) fashion (cf. Fig. 21.4A and B, respectively). In principle, the lateral concept does not differ much from an RGB display made of OLEDs—it only lacks the complex driving circuitry. The vertical stacking of OLEDs is feasible only for vacuum-based processes, as they allow the nondestructive additive deposition of as many layers as are needed. In contrast to these multiple-unit concepts, white light also can be generated in a single layer, as shown in Fig. 21.4C. Typically, an OLED EML has a thickness of 20–40 nm. Thicker layers are not feasible because nondoped layers would strongly increase resistive losses. Within these 20–40 nm, many concepts have been developed to realize white light. A crucial limitation of color mixing is the fact that the region within the EML where excitons are generated is usually only a few nanometers broad, and often close to one of the interfaces to adjacent layers (Reineke et al., 2007). Thus, often the volume in which the exciton distribution to various emitters needs to take place is severely restricted. Clearly, one way to realize white light is to divide the EML into sublayers, wherein each of them is containing one of the RGB emitters (Reineke et al., 2009). Alternatively, all emitters can be

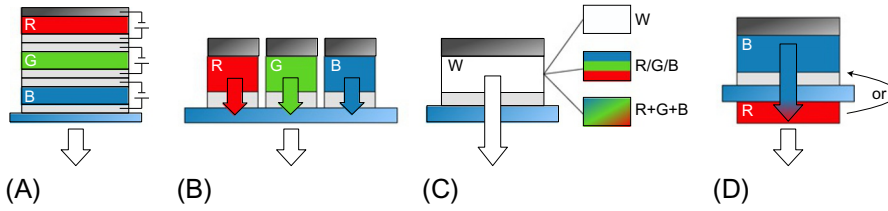

Fig. 21.4 Schematic illustrations of various concepts to realize white OLEDs. (A) Vertical stacking of RGB monochrome devices, (B) lateral structuring of RGB pixels, (C) single-unit white OLEDs, and (D) white-light generation through a combination of blue EL and at least one color conversion layer. For the single unit concept in (C), there are again various ways to generate white light in the EML. *W*, white-emitting material; *R*/*G*/*B*, sublayers for the primary colors; $R + G + B$, mixing of all emitters in one layer.
Source: SR/IAPP.

mixed into one common layer (D'Andrade et al., 2004); however, here, the respective concentrations of the emitters need to be optimized carefully, as the distribution of excitons among the different emitters is strongly affected by nonradiative energy transfer processes. Through careful material design, single-emitter while EL can be realized. Here, one type of emitter actually shows two spectrally distinct emitting states: one monomeric and one excimeric. When carefully adjusting the ratio of monomer and excimer emission bands, white light is possible with high efficiency (D'Andrade et al., 2002; Cocchi et al., 2007, 2009). For completeness, white light can be generated from a combination of a high-energy EL (blue) and color-conversion layers, that down-convert part of the primary EL spectrum to compose white light (Gohri et al., 2011), as shown in Fig. 21.4D.

It is important to note that, while the previous discussion centered on mixing the EL of RGB emitters, of course white light also can be generated by only two colors, which show CIE coordinates that cross the desired white color point on the Planckian locus on a straight connecting line (cf. Fig. 21.2; Fries et al., 2017; Springer et al., 2016; Su et al., 2008; Krotkus et al., 2016). Often, however, the CRI of two such color devices trails their three emitter analogs. On the other extreme, to generate white light with even higher CRIs, four emitter concepts have been proposed (Rosenow et al., 2010; Jou et al., 2013).

The generation of white light based on polymeric materials cannot be realized easily using the vertical stacking approach (cf. Fig. 21.4A), as the fabrication of multiple units on top of each other currently is impossible with wet-processing techniques. Here cross-linking and orthogonal processing limit the device's design freedom. On the other hand, the lateral concept (cf. Fig. 21.4B) is perfectly suited, especially for inkjet-printing techniques. Polymers with their inherent large physical size compared to small molecules have a number of advantages to realize white light "by (polymer) design." Here, polymers are developed that either comprise various chromophores in a main polymer backbone (Tu et al., 2004; Lee et al., 2015) or utilize a copolymer architecture with chromophores in main- and side-chain positions (Liu et al., 2007). All these polymer concepts can be realized with precise stoichiometric compositions, which guarantees good control of the additive color mixing of various emitter subsystems (chromophores).

21.3 Efficiency considerations

Optimizing the efficiency of a given light source is of utmost importance for two reasons: (1) only respectful and conservative use of energy will allow a future that tries to avoid negative impacts on our environment, and (2) many electronic devices and applications become portable or small (or both), where an increased power consumption will strongly hamper their time of use in a disconnected fashion. The OLED efficiency, therefore, is one of the key parameters that triggered the decades-long research up to now and will remain to be the central driving force for more research efforts.

21.3.1 Parameters influencing the efficiency

The external quantum efficiency (EQE) of an OLED, which is the most representative performance indicator quantity when comparing differently emitting OLEDs (Reineke et al., 2013), as it gives the ratio of extracted photons over injected charges. The other often-used performance indicator quantities are current efficiency (given in candelas per ampere) and luminous efficacy (given in lumens per watt), which both factor in the human eye response function and thus cannot be used to compare OLEDs with different EL spectra directly. The EQE can be expressed as the product of four main influencing parameters:

$$\eta_{\mathrm{EQE}} = \gamma \cdot \eta_{\mathrm{rad,\ eff}} \cdot \eta_{\mathrm{S/T}} \cdot \eta_{\mathrm{out}} \tag{21.1}$$

The first factor, γ, represents electrical efficiency. It accounts for injected charge carriers that do not contribute to recombination through the formation of excitons. Often, this factor is also referred to as *charge balance,* and it directly depends on the transport properties of the multilayer devices. Still, mostly determined indirectly from the discussion of the remaining parameters influencing η_{EQE}, the electrical efficiency is close to unity in optimized OLEDs (Adachi et al., 2001b; Erickson and Holmes, 2011, 2014). Furthermore, $\eta_{\mathrm{rad,\ eff}}$—the second factor in Eq. (21.1)—accounts for the effectiveness of a certain emitter. It treats the competition between the radiative and nonradiative rates of the emitting state that is utilized in a given emitter, which can be either a singlet or a triplet state, and hence the actual definition of $\eta_{\mathrm{rad,\ eff}}$ depends on the system. This parameter is called *effective radiative quantum efficiency* because it also accounts for possible enhancements of the radiative rates through the optical environment (Amos and Barnes, 1997)—that is, the OLED forms a thin-film optical cavity (Furno et al., 2012; Brütting et al., 2013). The third factor, $\eta_{\mathrm{S/T}}$, accounts for the share of excitons that are able to decay radiatively due to the quantum-mechanics spin selection rules. It will be discussed further in Section 21.3.2. The electrical efficiency, the effective radiative efficiency, and the spin factor can be summarized to the internal quantum efficiency as $\eta_{\mathrm{int}} = \gamma \cdot \eta_{\mathrm{rad,\ eff}} \cdot \eta_{\mathrm{S/T}}$, which describes the efficiency of photon generation of an emitter for the case of EL. The final factor, η_{out}, is the outcoupling efficiency. It depends on the optical environment and, as more recently was discovered, on the orientation of the transition dipole moment of the emitter molecules. A discussion of η_{out} will be given in Section 21.3.3.

21.3.2 Exciton spin

EL in OLEDs is realized through the recombination of uncorrelated electrons and holes to form an intermediate, neutral state—the exciton. OSCs, with their low degree of order and their low dielectric constants, typically possess very localized, Frenkel-type excitons. Their localization leads to the occurrence of energetically distinct spin manifolds for the excitons in form of singlet and triplet states. These are energetically split, with typical energy splittings in the range of few 100 meV (Reineke and Baldo, 2014), and show radiative recombination typically only from the singlet state

(Turro et al., 2010). This process is referred to as *fluorescence*. The radiative recombination from the triplet state, called *phosphorescence*, is very unlikely, as it requires a spin flip (Turro et al., 2010).

Before recombination, the respective electrons and holes are completely uncorrelated, so that the pairing of the two charge-carrier spins (fermions with spin-half) to one bosonic exciton is a truly statistical process. As the triplet states of organic molecules are threefold degenerate, there are three possibilities to form a triplet for each singlet state, with the result that in such uncorrelated systems, about 75% of the excitons come to life as triplets (Baldo et al., 1998; Segal et al., 2003; Burrows et al., 2001; Reineke and Baldo, 2012). Thus, if a conventional fluorescent material is used in OLEDs as the emitter, the internal quantum efficiency $\eta_{\text{int, F}}$ will be approximately only 25%, as all triplets formed decay nonradiatively (cf. Fig. 21.5). Already in the early years of OLED research, this limit has been considered a roadblock for the success of OLEDs.

Nowadays, it is clear that this limitation has been overcome by innovative molecular designs particularly made for OLEDs. The first concept is based on the realization of emitters with efficient and device-compatible phosphorescence (Baldo et al., 1998). This is achieved using organometallic complexes, where central heavy metals like iridium, platinum, and osmium introduce strong spin-orbit coupling (SOC) (Thompson, 2007). This SOC significantly speeds up the radiative phosphorescence rate—outcompeting nonradiative channels—and at the same time, it accelerates the intramolecular intersystem crossing (ISC) from singlet to triplet states (Yersin, 2004). The latter effect leads to the complete population of the material's triplet state,

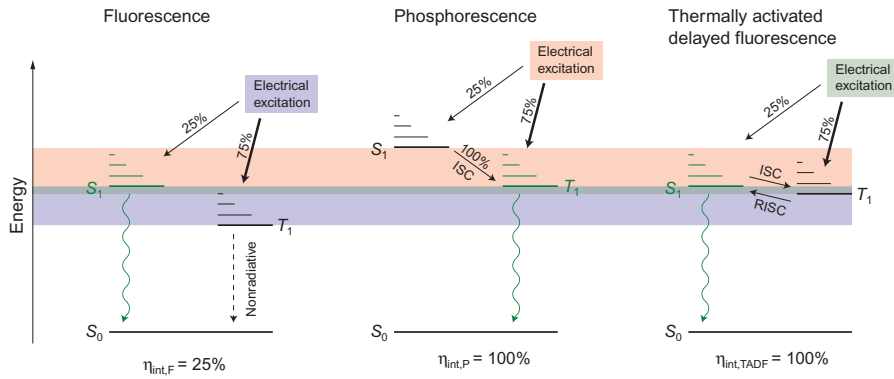

Fig. 21.5 Simplified energy diagrams to achieve equal emission energies for the important three emitter types used in OLEDs: fluorescence, phosphorescence, and TADF. S_0 represents the molecular ground state, S_1 and T_1 are the respective first excited singlet and triplet states, and $\eta_{\text{int, }i}$ represents the internal quantum efficiencies. The different colors indicate the respective energetic ranges, which are excited through the formation of excitons under electrical excitation.
Source: SR/IAPP.

which is an effective luminescent state. Consequently, under electrical excitation, this molecular concept leads to internal efficiencies topping at $\eta_{\text{int, P}} = 100\%$ (cf. Fig. 21.5) (Adachi et al., 2001b; Kim et al., 2013b).

As an alternative to organometallic phosphorescence, thermally activated delayed fluorescence (TADF) (cf. Fig. 21.5) allows for internal quantum efficiencies ($\eta_{\text{int, TADF}} = 100\%$) approaching unity as well (Endo et al., 2009; Uoyama et al., 2012). This excitonic concept does not need the complex organometallic chemistry; rather, it unfolds on a specifically optimized molecular design. The essence of TADF is the possibility of triplet states to upconvert to radiative singlet states via reverse ISC (RISC) with the assistance of thermal energy at room temperature (cf. Fig. 21.5). To do so, the energetic splitting between singlet and triplet states must be strongly reduced to be comparable to thermal energy (25 meV). As this is an energetically uphill process, it is slower than the radiative rates of the fluorescence, so TADF is accompanied by a delayed fluorescence component—hence the name—which shows identical spectral distribution compared to the prompt fluorescence. This is realized by constructing intramolecular donor-acceptor (DA) systems that lead to the formation of intramolecular charge-transfer excitons, where, due to the spatial separation, the energetic splitting strongly decreases and often reaches conditions where singlet and triplet configurations are energetically indistinguishable (Wong and Zysman-Colman, 2017). The same effect can be realized by constructing intermolecular interfaces of DA-type molecules, which leads to TADF emissions from the so-called exciplex state (Goushi et al., 2012). It is fair to note that while most of the efforts concentrate on purely organic TADF emitter development, the same excitonic properties can be achieved based on organometallic chemistry (Deaton et al., 2010).

The internal limits of conventional fluorescence ($\eta_{\text{S/T, F}} = 25\%$) can be overcome by utilizing a nonlinear excitonic process. Triplet-triplet annihilation (TTA)—that is, the collision of two triplet excitons—can lead to a contribution of upconverted singlet states. This process can increase the internal quantum efficiency to $\eta_{\text{S/T, F+TTA}} = 62.5\%$ (Kondakov et al., 2009), which is significantly higher than conventional fluorescence, but still far smaller than either phosphorescence or TADF.

Fig. 21.5 compares schematically the energy diagram for fluorescent, phosphorescent, and TADF emitters, where the emitting state is always kept at the same energy (singlet state for fluorescence and TADF, triplet state for phosphorescence). The different-shaded boxes indicate the energetic spectra that are excited under electrical excitation. Clearly, the phosphorescent emitter will have to carry the highest energy states (25% by share as a consequence of the spin statistics), which are consequently redirected to the triplet manifold. By raising the triplet energy of a TADF emitter closer to the singlet state, the conventionally lost 75% triplet states can be harvested, but equally important, the maximum energetic load on the emitter does not differ compared to the fluorescent emitter. This is an important point, as the only industrially relevant blue emitters to date are fluorescent. Neither phosphorescence nor TADF has been convincingly reported to realize stable and high-efficiency OLEDs, but clearly based on the previous arguments, TADF seems to have the better energetics at play to realize long-lived blue OLEDs.

21.3.3 Light outcoupling

The factor influencing the EQE of OLEDs with the largest margin for improvement is the outcoupling efficiency η_{out}. In very simple words, the thin-film-layered architecture of OLEDs turns them into weak optical cavities. The organic layers have refractive indices in the range of $n_{org} \approx 1.6 - 1.8$, which is higher than the respective values of the substrates used (glass or plastic, $n_{sub} \approx 1.5$), and especially the desired outcoupling medium, air ($n_{air} = 1.0$). This optical environment leads to a significant confinement of optical modes within the structure. As a rule of thumb, only about 20%–30% of the internally generated photons leave the device to the observer hemisphere in standard device layouts (bottom emission) (Greenham et al., 1994), clearly indicating that there is much room for improvement.

The light is generated in a high-refractive-index region and, thus, the differences in refractive indices introduce optical interfaces where total internal reflection (TIR) will occur, trapping part of the light in so-called guided internal modes.

To account properly for the complexity of state-of-the-art multilayer OLEDs, the light generated by the emitter molecules within the device is described by classical radiating dipoles (Neyts, 1998; Furno et al., 2012). Then their field propagation and power distribution in the optical structure (the OLED) are modeled by a driven damped oscillator to ultimately calculate the far-field emission pattern after passing the various optical interfaces. Now such models can even account for a combination of thin-film layers and thick optically transparent regions, which the substrates typically are. In contrast to the thin-film layered structure, which is treated as a coherent system, the latter exceeds the coherence length and is described by ray optics (Kovačič et al., 2018). Due to the rotational symmetry of the planar cavity structure, the description of the classical radiating dipole model is developed as a function of the in-plane wavevector $k_{\|}$ (cf. Fig. 21.6). Often, this vector is used in its normalized representation $k_{\|}/k$, where k is the wave vector within the emission layer. Consequently, $k_{\|}/k = 1$ corresponds to a propagation of the light in the plane of the layered structure.

Fig. 21.6 (center, right) shows the optical modes of a green phosphorescent OLED based on the emitter Ir(ppy)$_3$. For $\frac{k_{\|}}{k} < \frac{n_{air}}{n_{emitter}}$, light can escape the layered structure, which represents the useful portion of the radiated power generated in the OLED. Due to the optical interfaces in the complete OLED stack, different waveguided modes occur. First, for $\frac{n_{air}}{n_{emitter}} < \frac{k_{\|}}{k} < \frac{n_{sub}}{n_{emitter}}$, light is trapped inside the substrate (for $n_{air} < n_{sub} < n_{emitter}$). With increasing in-plane wave vector spanning $\frac{n_{sub}}{n_{emitter}} < \frac{k_{\|}}{k} < 1$, the so-called organic or waveguide modes occur, wherein light is trapped in the organic layer stack. For normalized in-plane wave vectors exceeding 1 (i.e., $\frac{k_{\|}}{k} > 1$), the light couples to evanescent modes in the form of excitation of metal surface plasmon polariton (SPP) modes with imaginary out-of-plane wave vector k_z. It is important to consider the interaction of the emitting dipoles with the various modes available. The respective coupling strength affects the excited-state lifetimes of the emitter molecules. This phenomenon is known as the *Purcell effect* (Purcell

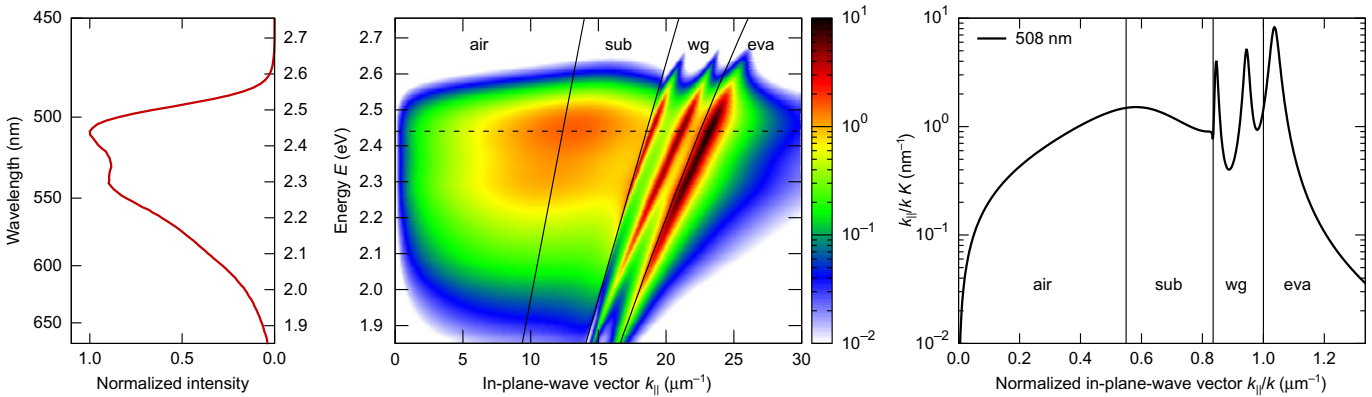

Fig. 21.6 Calculated power dissipation spectra (center) of a typical bottom-OLED with $Ir(ppy)_3$ as emitter. Here, the power dissipation spectra were weighted with the corresponding PL spectrum of the emitter (left). A cross section (right) at $\lambda = 508\,\text{nm}$ shows dissipated power into air, substrate (sub), waveguided modes (wg), and evanescent modes (eva). For determining the outcoupling efficiency the power dissipation spectra is integrated over the wavelength contributions, and then the ratio of outcoupled to total power is calculated.
Source: PAW/IAPP.

et al., 1946; Furno et al., 2012; Brütting et al., 2013). The complete power dissipation spectrum is a function of the wavelength (cf. Fig. 21.6, center), so that the correct treatment of the OLED optics requires the integration of the power dissipation spectrum and its weighting with the emission spectrum of the emitter (cf. Fig. 21.6, left). Whenever photons are generated at various vertical positions within the OLED stack (e.g., stacked and white OLEDs), their respective positions need to be considered correctly. Based on this optical modeling of OLEDs, the outcoupling efficiency of OLEDs can be computed, and further, the relative power per mode can be determined. This analysis is of key importance for the development of designs for increased light outcoupling.

For the green $Ir(ppy)_3$-based device, Fig. 21.7 (top center) shows the simulated EQE in dependence on ETL and HTL thickness. Here, the calculation considers a realistic radiative efficiency of the emitter of $\eta_{rad} = 0.8$ (Kawamura et al., 2005) (i.e., nonradiative losses of the emitter are considered). The four distinct positions with maximal EQE are a consequence of the optical cavity that supports different resonant wavelengths depending on the overall thickness between the reflecting interfaces. So clearly, optimum conditions for a respective emitter spectrum appear and will differ depending on the emission spectrum of the material. Consequently, the thickness optimization for differently emitting OLEDs always needs to be considered carefully. Furthermore, Fig. 21.7 (top right) shows the calculated photon fractions of the different modes as a function of the ETL thickness, while the HTL is set to approximately 43 nm. While the EQE exhibit strong thickness dependence, the coupled power into the substrate stays relatively constant over the ETL thickness. It is interesting to note that the optimal ETL thicknesses for the highest value of the summed contribution of air and substrate modes is increased, which becomes important for the optimal use of external outcoupling structures (Kovačič et al., 2018). As expected, the coupling to the waveguide modes increases significantly with increasing thickness, as the cavity can support more and more waveguide modes. On the contrary, the evanescent modes significantly decrease with increasing ETL thickness. Here, the increasing space between emitting dipoles and metal layers strongly suppresses coupling to the SPP modes (Reineke et al., 2009).

One effect on OLED optics not discussed so far is the emitter orientation. Recent reports have discovered that many organic material systems are not isotropically oriented in thin films, despite their typical amorphous nature (Yokoyama et al., 2010, 2008; Frischeisen et al., 2010). The orientation of the emitting dipoles has a strong impact on the overall device optics. Here, vertical oriented dipoles couple only weakly to the escape cone of an OLED, whereas dipoles oriented horizontally are the ideal photon sources when embedded in OLED stacks. The mode distribution of the $Ir(ppy)_3$-based OLED is shown in the top panel of Fig. 21.7. Here, the calculation considers a realistic radiative efficiency of the emitter of $\eta_{rad} = 0.8$ (Kawamura et al., 2005) (i.e., nonradiative losses of the emitter are considered) and isotropically distributed dipole sources (orientation factor $a = 1/3$). The bottom panel of Fig. 21.7 is calculated based on two important changes: First, the nonradiative losses of the emitter have been turned off to demonstrate an upper limit for the mode distribution; and, second, the emitter orientation is set to be preferentially horizontal ($a = 0$).

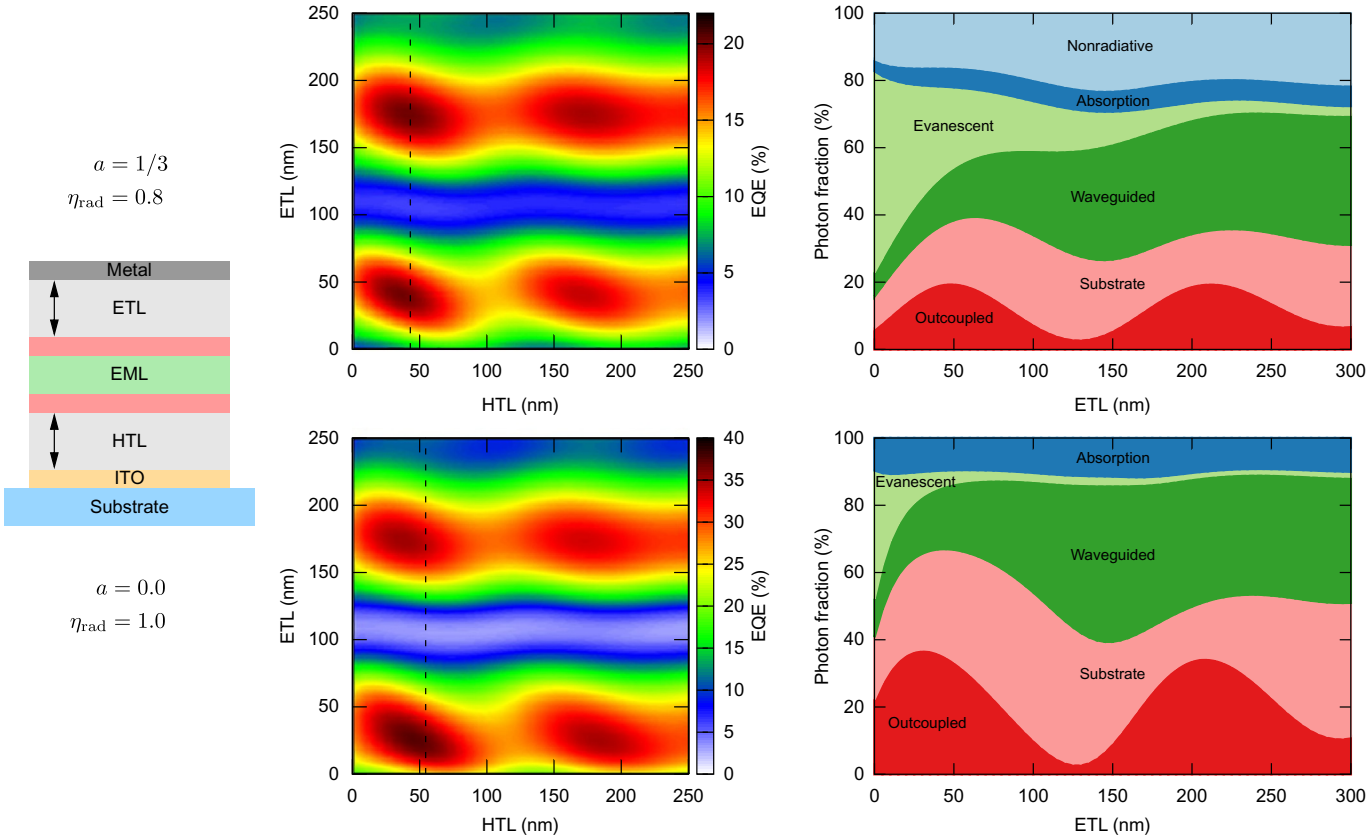

Fig. 21.7 Calculated EQE in dependence on ETL and HTL thickness and optical loss channels for a $Ir(ppy)_3$ bottom-OLED with realistic (top row) and ideal (bottom row) radiative efficiency and emitter orientation.
Source: PAW/IAPP.

Comparing the outcoupled fractions for both scenarios shows almost a twofold increase for the horizontally oriented emitter, with the radiative efficiency set to unity. This corresponds to about 40% EQE, when the cavity is optimized. Note that the optimal ETL and HTL layer thickness is changed. Experimentally, such an EQE has been demonstrated with a crystalline EML material that ensures a very high degree of horizontal orientation (Kim et al., 2016).

21.4 Applications

Based on the first devices reported, OLEDs were initially seen as a highly promising next-generation display technology. Soon afterward, they were suggested for use in general lighting. While these uses are vastly different, they share a similar device platform to the one previously described. However, the requirements to their emitted color, their luminance during use, and their lateral dimensions strongly differ, so these major research and development efforts are separated these days.

21.4.1 Displays

The technology to be replaced by OLEDs in the display sector are liquid crystal displays (LCDs), which have revolutionized the market penetration of displays as a whole and especially paved the way for the development of mobile displays. In contrast to LCDs, the biggest advantage of OLEDs is that they represent a self-emitting pixel technology (i.e., each pixel is generating the light individually). This difference allows for a significant reduction of the thickness (and thus the weight) of the overall display because no backlight is needed. It also supports true back content, as instead of blocking the backlight through cross-polarizers in case of LCDs the respective pixel is turned off. Ultimately, OLEDs are considered to be more power-conservative than LCD solutions.

Displays need to reproduce as many of the possible colors that the human eye can capture to allow the most realistic depiction of natural objects. The perception of color can be described by a color chart—namely, the CIE 1931 color space, defined by the Commission International de l'Eclairage (CIE) as shown in Fig. 21.3 for a 2-degree standard observer. In general, the term *light* refers to electromagnetic radiation with a wavelength within 380–780 nm. Here, monochromatic emission of a single wavelength is defining the outer rim (i.e., a horseshoe) of the diagram. Mixed colors, depending on their spectral distribution, are localized in the space opened up by the monochrome colors. Interestingly, different spectral distributions can result in identical color perceptions, a phenomenon called *metamerism*. Therefore, display technologies are designed to come as close to reality as possible, where the best compromise jointly for various display technologies is the use of three primary colors: red, green, and blue, opening up a color triangle in the CIE 1931 diagram. Thus, the primary pixel colors define the composition of possible colors by mixing the RGB colors accordingly. Here, the increase of the color triangle formed by red, green, and blue pixels will lead to wider coverage of the color gamut and allow for better overall color

reproduction. In comparison to the NTSC color standard (Livingston, 1954), typical EL spectra of OLEDs are shown in Fig. 21.3, with their respective locations in the CIE 1931 color space. The composition of images from individually addressable primary colors (RGB) is realized by laterally integrating RGB pixels with a high-enough density that ideally cannot be resolved by the observer, who in contrast views a seamless lateral distribution of colors.

The power consumption of a display can be decoupled from the primary optimization of display parameters that are associated with the image quality. Here, energy efficiency of a display enters the space of specifications to be optimized whenever the display usage must cope with limited power supply, as is the case in the fields of mobile displays that are part of small, off-grid packages. Ultimately, when for all primary colors, the most efficient OLEDs, operating at internal quantum efficiencies close to unity (cf. Section 21.3), are arranged in a display, OLED displays are more energy efficient than LCDs. However, the benefit in energy efficiency alone is not enough to allow a general transition from LCDs to OLEDs.

The self-emitting nature of OLED pixels are important not only for the abovementioned high-contrast achieved using true-black pixels, but also more naturally allow a wide viewing angle because the OLED emission approximately follows a Lambertian intensity distribution (Tanaka et al., 2007). In addition to these two important image quality aspects, the OLED fabrication is compatible with display architectures that support conformable and flexible substrates, which offers various new markets. Here, the OLED as the pixel technology is only a small part of the complete system, where the backplane is by far harder to develop for such flexible displays. The OLED itself is made of comparably soft materials (i.e., organic amorphous molecules), and is also very thin compared to the desired curvature radius of a flexible display, so that it is not representing the limiting factor.

The quality of the established LCDs is already so high that OLEDs need to follow current developments in display resolution, while at the same time not compromising the manufacturing yield. Current small mobile displays made from OLEDs at the eye-to-display distances typical for handheld devices are at >500 pixels-per-inch (ppi) (Soneira, 2018), which is beyond the resolution that the human eye can perceive (Banks et al., 1987; Campbell and Green, 1965; Campbell and Gubisch, 1966), in the range of 300–400 ppi. These resolutions are achieved with shadow-mask techniques with vacuum-deposited OLEDs. This trend to higher and higher resolutions put an increased focus on the OLED-to-backplane integration, while the OLED stacks become a smaller and smaller part of the whole process and system. This in turn calls for very robust and simplified stack designs. For instance, it is desired for OLED displays to develop RGB subpixels that share common layers (e.g., transport and blocking layers), as the complex lateral structuring into RGB subunits can be reduced to the color-defining layers only. Even higher pixel densities (exceeding 2000 ppi) are needed for virtual reality (VR) and augmented reality (AR) applications (Fujii et al., 2018), as those displays are located much closer to the eye.

An alternative concept, used often for large display panels, is the combination of a uniform white OLED architecture that is complemented with RGB color filters with

spatial resolution to realize the primary colors. Often, a fourth segment per unit cell is left unfiltered to allow a white pixel, leading to an RGBW display design. Especially on large area panels, this approach has advantages in the process yield.

21.4.2 Solid-state lighting

The challenges for OLEDs developed as general light sources (SSL) are quite contrary to the ones in the display sector. General lighting needs white-light emitting sources, so that here, the OLED development needs to find efficient solutions made from individual primary colors. This is because, while OLED emitters produce an EL spectra with large full-width at half-maximum (FHWM) in the range of 50–100 nm (cf. Fig. 21.3) (Reineke et al., 2010), that is not enough to span the visible part of the electromagnetic spectrum. Fig. 21.3 shows two important color compositions (color points E and A in the CIE 1931 diagram) from primary RGB spectra that resemble white light.

In contrast to OLED displays, solutions for SSL are single, large-area pixel concepts that do not need lateral structuring. Here, the challenge is the effective scaling to large areas, which is needed to realize white OLEDs with high-enough lumen output to allow their use as light sources. Structuring of OLED systems for SSL can become interesting only whenever the light source should sport the ability to vary its color to accommodate different user settings (Krotkus et al., 2016). The target for high lumen output can be achieved through increases in surface area or surface brightness, which both come with disparate technological hurdles. The increase in active OLED surface increases the physical size of the light source, which face problems in their installment the further the active size deviates from spot lights like lightbulbs. Additionally, large OLEDs need sophisticated solutions to distribute the charge carriers in the electrodes laterally (e.g., by metal grids), as otherwise, the emitting surface would be inhomogeneous and even self-heating effects may arise (Fischer et al., 2014). Increasing the surface brightness on the contrary negatively affects the device stability. The latter scales inversely with the device brightness (cf. Section 21.5.3). In reality, a good compromise between both parameters often needs to be found and is highly dependent on the respective application scenario.

What is currently one of the most important challenges for OLEDs for SSL is its price target. While displays are comparably high price sectors, especially in the television market, general lighting does not allow new technologies with a large premium in price. Considering a white LED retrofit lightbulb as a good price reference, it currently has a price of only a few cents per lumen in the retail market ($10–$20 for a 1000-lm lightbulb). In comparison, white OLEDs currently are more expensive by about a factor of 10 (Spindler et al., 2018). Here, the large area-light form factor of OLEDs introduces a secondary problem: With increasing surface area, the substrate scales accordingly, which may add significantly to the overall package price. Beyond the simple cost arguments, the form factor introduces barriers to a seamless market penetration. Whereas inorganic LEDs fit into widely accepted general lighting infrastructure in the form of retrofit bulbs and fluorescent tube form factors, OLEDs provide new opportunities in the SSL sector, especially in emerging niche markets.

21.4.3 Automotive sector

An emerging application field for OLEDs is the automotive sector, which suggests that it is an area with a high need for customization of light sources. Here, beyond delivering a high-quality user experience, the differentiation of the individual manufacturers through customized display and lighting solutions is key to future concept developments. There are four main areas, where OLEDs are intensively explored for use in automobiles: dashboard displays, head-up displays, interior ambient lighting, and exterior lights. Currently, many concepts are proposed for future dashboards, which heavily build on customized OLED displays. Here, the ability to produce such displays on conformable substrates offers a virtually seamless integration into the car interior, naturally following the topography of the dashboard design. The slim design of the OLED technology is important to allow the integration of displays on surfaces where the installation depth is limited. As OLEDs can be made transparent (Bulovic et al., 1996; Fries et al., 2017; Görrn et al., 2006), they are suggested for use in head-up displays for augmented reality functionality in the driver's field of view.

One important aspect here is the required brightness of such head-up solutions, which is much higher ($>10{,}000\,cd/m^2$) than many other applications to allow a contrast with the daylight background. While reaching these values is not a problem for OLEDs, their long-term stability is greatly reduced as the device's lifetime scales inversely with its brightness (cf. Section 21.5.3). The use of OLEDs as interior ambient lights is conceivable, but the degree of customization is very high, as the physical dimensions of such lights need to be defined specifically for each use. Current developments of interior design suggest that such solutions need to allow color tunability (Burrows et al., 1996; Kanno et al., 2006; Fröbel et al., 2015; Krotkus et al., 2016), including the generation of white light with different color temperatures. However, inorganic LEDs are much further developed currently and can be packaged to realize virtually similar effects and functionalities. OLEDs used as exterior lights have seen first demonstrations recently in small series and premium automobiles in form of rear lights (red color) (HELLA GmbH & Co. KGaA, 2018). These rear lights are currently supplemented with LED solutions for brake lights and turn indicators, as the brightness requirements are not met by OLEDs yet. Even with the current performance limitations, OLEDs are very attractive for the various automotive manufacturers, as they allow for a high degree of product differentiation.

The automotive sector is very attractive for OLEDs, as it offers gradual market penetration, tolerates a certain price premium—either over existing technologies or because it generates an added value—and represents a large market. For modern automotive lights including LEDs and also OLEDs, replacing the actual light source is no longer an option, because they are highly integrated into the complete light body. Therefore, OLEDs must meet lifetime performance values including immunity toward sudden death exceeding the average lifespan of an automotive. Importantly, the conditions are harsher compared to other usage scenarios (displays or SSL), especially because of the large range of possible temperatures ($-20°C$ to $110°C$ in the most extreme cases) and various humidity levels.

21.4.4 Niche markets

In addition to the applications mentioned previously, OLEDs offer unique features that make them attractive for various other fields of use. In particular, the flexibility in the device processing and the overall low-temperature fabrication are crucial aspects. Paired with the material softness (White et al., 2013), many applications in the medical sector become attractive. For instance, OLEDs can be used for light treatment in bandagelike systems (Samuel et al., 2015), where their low physical impact is of key importance for comfortable use on patients. Similarly, sensoric systems, where one or more light sources are needed for a photonic-based readout, can be made effectively with OLEDs (Krujatz et al., 2016; Lochner et al., 2014; Bansal et al., 2014). Furthermore, OLED microdisplays have been used recently to simulate and manipulate cells. Here, OLEDs are investigated as a novel platform for optogenetic research (Steude et al., 2016).

Also recently, OLEDs have been developed as an ultralow-cost technology for interactive signage solutions in the areas of print media and retail product packaging (INURU GmbH [WWW Document], 2018), where the overall lifespan specifications are comparably moderate. Here, printing is used as the processing of choice, which will allow for print-on-demand solutions and for lowest possible manufacturing costs.

In summary, on the shoulder of giants in the form of display and SSL developments, OLEDs are constantly being explored as light sources in new settings. Here, their use both as complete displays and individual segmented pixels is possible. What is a niche application today soon may become a mainstream solution.

21.5 Current research frontiers

OLED research started with the seminal work of Tang and VanSlyke (1987), demonstrating efficient EL from thin-film, organic-layered systems. The technology has matured since then, and products in the form of small and large displays have entered the broad consumer market. Still, the research field around the OLED technology is very active, where further optimization is needed and seems realistic. Answers to various scientific research questions remain to be found. At the same time, more consolidation of the technology will take place in the industrial sector. In this section, current research efforts will be discussed briefly.

21.5.1 Material development

Organic electronics in general is a research field with heavy efforts on material investigation and development, simply because there are so many possible compounds to consider (Reymond et al., 2011). Seen globally, this material freedom reduces the overall pace of progress, as it is a highly parallel effort where various classes of materials are developed independently. Machine learning is nowadays implemented into the material development process, especially for the purpose of accelerating the material screening (Gómez-Bombarelli et al., 2016). For both mainstream display

applications and SSL, the need for high efficiency and stable blue OLED material systems remains omnipresent. While blue phosphorescence clearly has the potential to realize the highest possible internal quantum efficiencies, the device stability is not sufficient for its full adoption, even after many years of research. One specific material development has recently emerged as an alternative to phosphorescence: TADF. Here, the hope is high that this material concept will allow fulfilling the specifications of high efficiency and stability, especially because the material space is much greater than with organometallic phosphorescence solutions (Wong and Zysman-Colman, 2017). Both material systems are being continuously investigated in parallel (Zhang et al., 2014; Nakanotani et al., 2013) to find a solution to one of the most pressing industrial problems.

If future applications call for higher operating brightness values by orders of magnitude (e.g., head-up or microdisplays), device stability becomes a more severe problem (cf. Section 21.5.3). Hence, further material research is likely to be an integral part of future efforts.

Currently, all mass-market and most pilot-production OLED systems are made using vacuum deposition techniques because this fabrication is easier to control and allows a higher degree of complexity with respect to the stack architecture. Yet at the same time, the production process as a whole is heavy on resources compared to solution-processing techniques like inkjet printing or other coating solutions. Here, all vacuum-processed devices in the respective applications (displays, signage, or SSL) serve as the performance standard, where the major material development task is to provide performance semiconductor materials that—together with their processing protocol (cf. Section 21.5.4)—allow for matching the current benchmarks. If this is achieved, it also will bring about a significant drop in production costs.

21.5.2 Scalable concepts for light-outcoupling

As discussed in Section 21.3.3, the limited share of photons that escape the thin-film structure have great potential for much-needed efficiency improvements. Here, simple arguments always suggest that two to three times the number of improvements are possible by harvesting most of the internal optical modes (cf. Fig. 21.7). However, while high improvements certainly are possible (Reineke et al., 2009; Jeon et al., 2015; Kim et al., 2013a), the respective realistic settings are often neglected, leading to many concepts and results that do not comply with industrial needs.

For displays, two aspects are crucial. First, most displays use OLEDs in top-emitting configurations, which is a different and much more complex optical problem. For instance, there are no substrate modes that one can utilize, and most of the light is trapped in organic mode (Hofmann et al., 2010; Thomschke et al., 2012). Second, the display technology cannot accept solutions that negatively affect the sharp pixel definition on the microscale, as this would introduce blurry images. Consequently, most of the concepts that use scattering or textured layers are not suited for use in displays. Considering these tight requirements, the twofold-to-threefold potential of OLEDs in concepts for enhanced light outcoupling does not seem to be a realistic target in the display sector.

For large-area SSL solutions, the requirements for successful outcoupling concepts are vastly different than for the display sector. OLEDs for large-area lighting are actually bottom-emitting devices. Here, optical solutions can indeed use scattering and textured layers and systems, as the far-field appearance of lighting tiles does not differ, and often light sources are used only in illuminating (i.e., indirect) settings. If lateral resolution is part of the device concept (Krotkus et al., 2016), such blurring optics can even be beneficial, as lateral light inhomogeneities are effectively mixed. What is important for these large-area systems is the scalability of possible concepts for enhanced light outcoupling. Therefore, the effect must be scalable (i.e., the enhancement must be given not only for lab-size OLED pixels, but equally for large lateral dimensions). At the same time, the fabrication for the outcoupling concept must be scalable to large areas, while ideally not significantly affecting the cost of fabrication of the complete package.

Section 21.3.3 showed that the emitter orientation can increase the EQE of an OLED significantly. This effect is so powerful because it is a truly intrinsic property of the materials used, so all the requirements for both displays and SSL are met. Clearly for displays, perfectly oriented emitters might prove to be the ideal target for future uses. Currently, understanding of the nanoscale effects leading to the orientation is developed, and—depending on the material and the processes involved—different explanations have been suggested (Mayr and Brütting, 2015; Jurow et al., 2016; Moon et al., 2017; Gather and Reineke, 2015). What is more important is to transfer this knowledge into concepts that will allow for controlling the orientation to exploit its potential fully. This is a truly nanoscale molecular engineering problem asking for interdisciplinary efforts. Another route to increase the light outcoupling while maintaining the undistorted pixel appearance needed for displays is the incorporation of a low refractive index (Fuchs et al., 2015; Watanabe et al., 2018) or birefringent functional layers (Callens et al., 2015) into the device stack to manipulate the mode distribution in favor for higher extracted modes.

21.5.3 Lifetime and failure

The lifetime of light sources has been an issue for users ever since artificial light entered our routines. Here, there are two clear cases: (1) the light intensity, quality, or both reduce over time, and (2) the light source abruptly fails. For OLEDs, this is no different. Fig. 21.8 (left) shows the luminance aging of a green-bottom-OLED comprising $Ir(ppy)_3$. When the device is operated at a constant current density of $j = 10\,mA/cm^2$, the luminance drops as a function of time and, often, the driving voltage increases at the same time. The device's lifetime, defined as the time to reach a certain value from the initial luminance (e.g., LT_{50} = time to reach 50% of the initial luminance), scales inversely with the device brightness (cf. Fig. 21.8, right) (Meerheim et al., 2006; Scholz et al., 2015). For displays, rather than the LT_{50} often used in academia, LT_{97} is the standard. For SSL, LT_{70} is mostly used by industry.

Aging effects of OLEDs have been studied using various approaches, and the sources for improvement are the material development on the one side, and the fabrication process, including packaging of the devices, on the other. The origins of

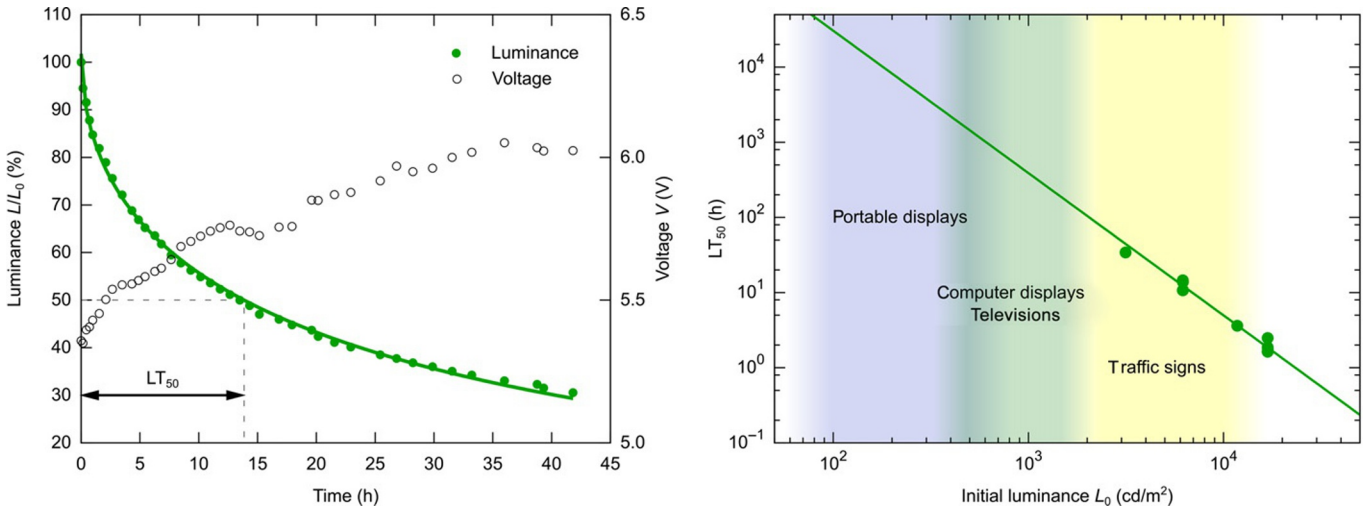

Fig. 21.8 Lifetime characteristics of a simplified two-layer, green-bottom OLEDs with $Ir(ppy)_3$ as emitting material under extended aging. Under a constant current density of $j = 10\,mA/cm^2$, the luminance drops and the voltage increases over time (left). The lifetime (e.g., LT_{50}) scales inversely proportional to the luminance defining application limits (right).
Source: PAW/IAPP.

device instabilities are highly material and package related, so that generalizations cannot be made.

Clearly, the lifetime of OLEDs is the most important device characteristic when it comes to possible use in commercial products. The lifetime specifications need to fit into the targeted application scenario (cf. Fig. 21.8, right), where limited stability currently disregards some potential fields of use.

21.5.4 Processing and integration

The materials (small molecules and polymers) and their possible fabrication methods open up a diverse setting for possible upscaling efforts. In the end, materials and processes need to fit perfectly together to obtain the best-performing OLED technology. However, the uncertainty in deciding which path allows the highest performance and profit often complicates the strategy development of leading industry. At the current stage, the processes are mostly vacuum- and small molecule-based, as this combination sets the benchmark for device efficiencies (and, more important, stability).

Clearly, the most interesting question will be how much and how fast solution-processing techniques that include the necessary materials can close the gap to vacuum technology. Being able to print high performance OLED products will be a game changer.

21.6 Outlook

OLEDs are the most successful functional device category of the diverse electronics based on OSC materials. This success is based on the fact that OLEDs build on a central property to which organic materials are very well suited: highly efficient luminescence. The transport properties needed to realize efficient EL are not demanding compared to other electronic devices like transistors. Conceptually, everything has been demonstrated using this device platform. The main challenge for the future is to overcome limitations in device stability—always seen in relation to the application in question—which can involve vastly different specifications. If this issue can be solved, the investment in broader production capacities will follow, which ultimately will lead to a significant cost reduction. Consequently, OLEDs will become a high-quality commodity, unmatched in many fields of use, that will be found everywhere in daily life.

References

Adachi, C., Baldo, M.A., Forrest, S.R., Lamansky, S., Thompson, M.E., Kwong, R.C., 2001a. High-efficiency red electrophosphorescence devices. Appl. Phys. Lett. 78, 1622–1624. https://doi.org/10.1063/1.1355007.

Adachi, C., Baldo, M.A., Thompson, M.E., Forrest, S.R., 2001b. Nearly 100% internal phosphorescence efficiency in an organic light-emitting device. J. Appl. Phys. 90, 5048–5051. https://doi.org/10.1063/1.1409582.

Amos, R.M., Barnes, W.L., 1997. Modification of the spontaneous emission rate of Eu^{3+} ions close to a thin metal mirror. Phys. Rev. B 55, 7249–7254. https://doi.org/10.1103/PhysRevB.55.7249.

Baldo, M.A., O'Brien, D.F., You, Y., Shoustikov, A., Sibley, S., Thompson, M.E., Forrest, S.R., 1998. Highly efficient phosphorescent emission from organic electroluminescent devices. Nature 395, 151–154. https://doi.org/10.1038/25954.

Banks, M.S., Geisler, W.S., Bennett, P.J., 1987. The physical limits of grating visibility. Vision Res. 27, 1915–1924. https://doi.org/10.1016/0042-6989(87)90057-5.

Bansal, A.K., Hou, S., Kulyk, O., Bowman, E.M., Samuel, I.D.W., 2014. Wearable organic optoelectronic sensors for medicine. Adv. Mater. 27, 7638–7644. https://doi.org/10.1002/adma.201403560.

Brütting, W., Frischeisen, J., Schmidt, T.D., Scholz, B.J., Mayr, C., 2013. Device efficiency of organic light-emitting diodes: progress by improved light outcoupling. Phys. Stat. Sol. A 210, 44–65. https://doi.org/10.1002/pssa.201228320.

Bulovic, V., Gu, G., Burrows, P.E., Forrest, S.R., Thompson, M.E., 1996. Transparent light-emitting devices. Nature 380, 29. https://doi.org/10.1038/380029a0.

Burroughes, J.H., Bradley, D.D.C., Brown, A.R., Marks, R.N., Mackay, K., Friend, R.H., Burns, P.L., Holmes, A.B., 1990. Light-emitting diodes based on conjugated polymers. Nature 347, 539–541. https://doi.org/10.1038/347539a0.

Burrows, P.E., Forrest, S.R., Sibley, S.P., Thompson, M.E., 1996. Color-tunable organic light-emitting devices. Appl. Phys. Lett. 69, 2959–2961. https://doi.org/10.1063/1.117743.

Burrows, H.D., Seixas de Melo, J., Serpa, C., Arnaut, L.G., Monkman, A.P., Hamblett, I., Navaratnam, S., 2001. S1∼>T1 intersystem crossing in π-conjugated organic polymers. J. Chem. Phys. 115, 9601–9606. https://doi.org/10.1063/1.1413969.

Callens, M.K., Yokoyama, D., Neyts, K., 2015. Anisotropic materials in OLEDs for high out-coupling efficiency. Opt. Express 23, 21128–21148. https://doi.org/10.1364/OE.23.021128.

Campbell, F.W., Green, D.G., 1965. Optical and retinal factors affecting visual resolution. J. Physiol. 181, 576–593. https://doi.org/10.1113/jphysiol.1965.sp007784.

Campbell, F.W., Gubisch, R.W., 1966. Optical quality of the human eye. J. Physiol. 186, 558–578. https://doi.org/10.1113/jphysiol.1966.sp008056.

Cocchi, M., Kalinowski, J., Virgili, D., Fattori, V., Develay, S., Williams, J.a.G., 2007. Single-dopant organic white electrophosphorescent diodes with very high efficiency and its reduced current density roll-off. Appl. Phys. Lett. 90, 163508. https://doi.org/10.1063/1.2722675.

Cocchi, M., Kalinowski, J., Fattori, V., Williams, J.A.G., Murphy, L., 2009. Color-variable highly efficient organic electrophosphorescent diodes manipulating molecular exciton and excimer emissions. Appl. Phys. Lett. 94, 073309. https://doi.org/10.1063/1.3086900.

Coehoorn, R., van Eersel, H., Bobbert, P., Janssen, R., 2015. Kinetic Monte Carlo study of the sensitivity of OLED efficiency and lifetime to materials parameters. Adv. Funct. Mater. 25, 2024–2037. https://doi.org/10.1002/adfm.201402532.

D'Andrade, B.W., Brooks, J., Adamovich, V., Thompson, M.E., Forrest, S.R., 2002. White light emission using triplet excimers in electrophosphorescent organic light-emitting devices. Adv. Mater. 14, 1032–1036. https://doi.org/10.1002/1521-4095(20020805)14:15<1032::AID-ADMA1032>3.0.CO;2-6.

D'Andrade, B.W., Holmes, R.J., Forrest, S.R., 2004. Efficient organic electrophosphorescent white-light-emitting device with a triple doped emissive layer. Adv. Mater. 16, 624–628. https://doi.org/10.1002/adma.200306670.

Deaton, J.C., Switalski, S.C., Kondakov, D.Y., Young, R.H., Pawlik, T.D., Giesen, D.J., Harkins, S.B., Miller, A.J.M., Mickenberg, S.F., Peters, J.C., 2010. E-type delayed fluorescence of a phosphine-supported $Cu_2(\mu\text{-}NAr_2)_2$ diamond core: harvesting singlet and triplet excitons in OLEDs. J. Am. Chem. Soc. 132, 9499–9508. https://doi.org/10.1021/ja1004575.

Endo, A., Ogasawara, M., Takahashi, A., Yokoyama, D., Kato, Y., Adachi, C., 2009. Thermally activated delayed fluorescence from Sn^{4+}–porphyrin complexes and their application to organic light emitting diodes—a novel mechanism for electroluminescence. Adv. Mater. 21, 4802–4806. https://doi.org/10.1002/adma.200900983.

Erickson, N.C., Holmes, R.J., 2011. Relating charge transport and performance in single-layer graded-composition organic light-emitting devices. J. Appl. Phys. 110, 084515. https://doi.org/10.1063/1.3653285.

Erickson, N.C., Holmes, R.J., 2014. Engineering efficiency roll-off in organic light-emitting devices. Adv. Funct. Mater. 24, 6074–6080. https://doi.org/10.1002/adfm.201401009.

Fan, C., Zhu, L., Jiang, B., Li, Y., Zhao, F., Ma, D., Qin, J., Yang, C., 2013. High power efficiency yellow phosphorescent OLEDs by using new iridium complexes with halogen-substituted 2-phenylbenzo[d]thiazole ligands. J. Phys. Chem. C 117, 19134–19141. https://doi.org/10.1021/jp406220c.

Fischer, A., Koprucki, T., Gärtner, K., Tietze, M.L., Brückner, J., Lüssem, B., Leo, K., Glitzky, A., Scholz, R., 2014. Feel the heat: nonlinear electrothermal feedback in organic LEDs. Adv. Funct. Mater. 24, 3367–3374. https://doi.org/10.1002/adfm.201303066.

Fleetham, T., Li, G., Wen, L., Li, J., 2014. Efficient "pure" blue OLEDs employing tetradentate Pt complexes with a narrow spectral bandwidth. Adv. Mater. 26, 7116–7121. https://doi.org/10.1002/adma.201401759.

Forrest, S.R., 2004. The path to ubiquitous and low-cost organic electronic appliances on plastic. Nature 428, 911–918. https://doi.org/10.1038/nature02498.

Fries, F., Fröbel, M., Lenk, S., Reineke, S., 2017. Transparent and color-tunable organic light-emitting diodes with highly balanced emission to both sides. Org. Electron. 41, 315–318. https://doi.org/10.1016/j.orgel.2016.11.022.

Frischeisen, J., Yokoyama, D., Adachi, C., Brütting, W., 2010. Determination of molecular dipole orientation in doped fluorescent organic thin films by photoluminescence measurements. Appl. Phys. Lett. 96, 073302. https://doi.org/10.1063/1.3309705.

Fröbel, M., Schwab, T., Kliem, M., Hofmann, S., Leo, K., Gather, M.C., 2015. Get it white: color-tunable AC/DC OLEDs. Light Sci. Appl. 4, e247. https://doi.org/10.1038/lsa.2015.20.

Fuchs, C., Will, P.-A., Wieczorek, M., Gather, M.C., Hofmann, S., Reineke, S., Leo, K., Scholz, R., 2015. Enhanced light emission from top-emitting organic light-emitting diodes by optimizing surface plasmon polariton losses. Phys. Rev. B. 92, 245306. https://doi.org/10.1103/PhysRevB.92.245306.

Fujii, T., Kon, C., Motoyama, Y., Shimizu, K., Shimayama, T., Yamazaki, T., Kato, T., Sakai, S., Hashikaki, K., Tanaka, K., Nakano, Y., 2018. 4032 ppi high-resolution OLED microdisplay. SID 2018 DIGEST 46-3, 613–616.

Furno, M., Meerheim, R., Hofmann, S., Lüssem, B., Leo, K., 2012. Efficiency and rate of spontaneous emission in organic electroluminescent devices. Phys. Rev. B. 85, 115205. https://doi.org/10.1103/PhysRevB.85.115205.

Gather, M.C., Reineke, S., 2015. Recent advances in light outcoupling from white organic light-emitting diodes. JPE 5, 057607. https://doi.org/10.1117/1.JPE.5.057607.

Gohri, V., Hofmann, S., Reineke, S., Rosenow, T., Thomschke, M., Levichkova, M., Lüssem, B., Leo, K., 2011. White top-emitting organic light-emitting diodes employing

a heterostructure of down-conversion layers. Org. Electron. 12, 2126–2130. https://doi.org/10.1016/j.orgel.2011.09.002.

Gómez-Bombarelli, R., Aguilera-Iparraguirre, J., Hirzel, T.D., Duvenaud, D., Maclaurin, D., Blood-Forsythe, M.A., Chae, H.S., Einzinger, M., Ha, D.-G., Wu, T., Markopoulos, G., Jeon, S., Kang, H., Miyazaki, H., Numata, M., Kim, S., Huang, W., Hong, S.I., Baldo, M., Adams, R.P., Aspuru-Guzik, A., 2016. Design of efficient molecular organic light-emitting diodes by a high-throughput virtual screening and experimental approach. Nat. Mater. Adv. 15, 1120–1127. https://doi.org/10.1038/nmat4717.

Görrn, P., Sander, M., Meyer, J., Kröger, M., Becker, E., Johannes, H.-H., Kowalsky, W., Riedl, T., 2006. Towards see-through displays: fully transparent thin-film transistors driving transparent organic light-emitting diodes. Adv. Mater. 18, 738–741. https://doi.org/10.1002/adma.200501957.

Goushi, K., Kwong, R., Brown, J.J., Sasabe, H., Adachi, C., 2004. Triplet exciton confinement and unconfinement by adjacent hole-transport layers. J. Appl. Phys. 95, 7798–7802. https://doi.org/10.1063/1.1751232.

Goushi, K., Yoshida, K., Sato, K., Adachi, C., 2012. Organic light-emitting diodes employing efficient reverse intersystem crossing for triplet-to-singlet state conversion. Nat. Photon 6, 253–258. https://doi.org/10.1038/nphoton.2012.31.

Greenham, N.C., Friend, R.H., Bradley, D.D.C., 1994. Angular dependence of the emission from a conjugated polymer light-emitting diode: implications for efficiency calculations. Adv. Mater. 6, 491–494. https://doi.org/10.1002/adma.19940060612.

Greiner, M.T., Helander, M.G., Tang, W.-M., Wang, Z.-B., Qiu, J., Lu, Z.-H., 2012. Universal energy-level alignment of molecules on metal oxides. Nat. Mater. 11, 76–81. https://doi.org/10.1038/nmat3159.

HELLA GmbH & Co. KGaA, 2018. HELLA lighting concept sets new standards in new Audi A8.

Hofmann, S., Thomschke, M., Freitag, P., Furno, M., Lüssem, B., Leo, K., 2010. Top-emitting organic light-emitting diodes: influence of cavity design. Appl. Phys. Lett. 97, 253308. https://doi.org/10.1063/1.3530447.

INURU GmbH [WWW Document], 2018. INURU Let there be light. https://www.inuru.de. (Accessed 26 May 2018).

Jeon, S., Lee, J.-H., Jeong, J.-H., Song, Y.S., Moon, C.-K., Kim, J.-J., Youn, J.R., 2015. Vacuum nanohole array embedded phosphorescent organic light emitting diodes. Sci. Rep. 5. https://doi.org/10.1038/srep08685.

Jou, J.-H., Hsieh, C.-Y., Tseng, J.-R., Peng, S.-H., Jou, Y.-C., Hong, J.H., Shen, S.-M., Tang, M.-C., Chen, P.-C., Lin, C.-H., 2013. Candle light-style organic light-emitting diodes. Adv. Funct. Mater. 23, 2750–2757. https://doi.org/10.1002/adfm.201203209.

Jurow, M.J., Mayr, C., Schmidt, T.D., Lampe, T., Djurovich, P.I., Brütting, W., Thompson, M.E., 2016. Understanding and predicting the orientation of heteroleptic phosphors in organic light-emitting materials. Nat. Mater. 15, 85–91. https://doi.org/10.1038/nmat4428.

Kanno, H., Giebink, N.C., Sun, Y., Forrest, S.R., 2006. Stacked white organic light-emitting devices based on a combination of fluorescent and phosphorescent emitters. Appl. Phys. Lett. 89, 023503. https://doi.org/10.1063/1.2219725.

Kawamura, Y., Goushi, K., Brooks, J., Brown, J.J., Sasabe, H., Adachi, C., 2005. 100% phosphorescence quantum efficiency of Ir(III) complexes in organic semiconductor films. Appl. Phys. Lett. 86, 071104. https://doi.org/10.1063/1.1862777.

Kawamura, Y., Brooks, J., Brown, J.J., Sasabe, H., Adachi, C., 2006. Intermolecular interaction and a concentration-quenching mechanism of phosphorescent Ir(III) complexes in a solid film. Phys. Rev. Lett. 96, 017404. https://doi.org/10.1103/PhysRevLett.96.017404.

Kim, J.-B., Lee, J.-H., Moon, C.-K., Kim, S.-Y., Kim, J.-J., 2013a. Highly enhanced light extraction from surface plasmonic loss minimized organic light-emitting diodes. Adv. Mater. 25, 3571–3577. https://doi.org/10.1002/adma.201205233.

Kim, S.-Y., Jeong, W.-I., Mayr, C., Park, Y.-S., Kim, K.-H., Lee, J.-H., Moon, C.-K., Brütting, W., Kim, J.-J., 2013b. Organic light-emitting diodes with 30% external quantum efficiency based on a horizontally oriented emitter. Adv. Funct. Mater. 23, 3896–3900. https://doi.org/10.1002/adfm.201300104.

Kim, K.-H., Liao, J.-L., Lee, S.W., Sim, B., Moon, C.-K., Lee, G.-H., Kim, H.J., Chi, Y., Kim, J.-J., 2016. Crystal organic light-emitting diodes with perfectly oriented non-doped Pt-based emitting layer. Adv. Mater. 28, 2526–2532. https://doi.org/10.1002/adma.201504451.

Koch, N., 2007. Organic electronic devices and their functional interfaces. ChemPhysChem 8, 1438–1455. https://doi.org/10.1002/cphc.200700177.

Kondakov, D.Y., Pawlik, T.D., Hatwar, T.K., Spindler, J.P., 2009. Triplet annihilation exceeding spin statistical limit in highly efficient fluorescent organic light-emitting diodes. J. Appl. Phys.. 106124510https://doi.org/10.1063/1.3273407.

Kotadiya, N.B., Lu, H., Mondal, A., Ie, Y., Andrienko, D., Blom, P.W.M., Wetzelaer, G.-J.A.H., 2018. Universal strategy for Ohmic hole injection into organic semiconductors with high ionization energies. Nat. Mater. 1. https://doi.org/10.1038/s41563-018-0022-8.

Kovačič, M., Will, P.-A., Lipovšek, B., Topič, M., Lenk, S., Reineke, S., Krč, J., 2018. Coupled optical modeling for optimization of organic light-emitting diodes with external outcoupling structures. ACS Photonics 5, 422–430. https://doi.org/10.1021/acsphotonics.7b00874.

Krotkus, S., Kasemann, D., Lenk, S., Leo, K., Reineke, S., 2016. Adjustable white-light emission from a photo-structured micro-OLED array. Light Sci. Appl. 5, e16121. https://doi.org/10.1038/lsa.2016.121.

Krujatz, F., Hild, O., Fehse, K., Jahnel, M., Werner, A., Bley, T., 2016. Exploiting the potential of OLED-based photo-organic sensors for biotechnological applications. Chem. Sci. J. 7. https://doi.org/10.4172/2150-3494.1000134.

Lee, S.Y., Yasuda, T., Nomura, H., Adachi, C., 2012. High-efficiency organic light-emitting diodes utilizing thermally activated delayed fluorescence from triazine-based donor–acceptor hybrid molecules. Appl. Phys. Lett.. 101093306. https://doi.org/10.1063/1.4749285.

Lee, S.K., Hwang, D.-H., Jung, B.-J., Cho, N.S., Lee, J., Lee, J.-D., Shim, H.-K., 2015. The fabrication and characterization of single-component polymeric white-light-emitting diodes. Adv. Funct. Mater. 15, 1647–1655. https://doi.org/10.1002/adfm.200500060.

Lee, J., Chen, H.-F., Batagoda, T., Coburn, C., Djurovich, P.I., Thompson, M.E., Forrest, S.R., 2016. Deep blue phosphorescent organic light-emitting diodes with very high brightness and efficiency. Nat. Mater. 15, 92–98. https://doi.org/10.1038/nmat4446.

Li, G., Fleetham, T., Turner, E., Hang, X.-C., Li, J., 2014. Highly efficient and stable narrow-band phosphorescent emitters for OLED applications. Adv. Opt. Mater. 3, 390–397. https://doi.org/10.1002/adom.201400341.

Liu, J., Xie, Z.Y., Cheng, Y.X., Geng, Y.H., Wang, L.X., Jing, X.B., Wang, F.S., 2007. Molecular design on highly efficient white electroluminescence from a single-polymer system with simultaneous blue, green, and red emission. Adv. Mater. 19, 531–535. https://doi.org/10.1002/adma.200601580.

Liu, J., Jiang, M., Zhou, X., Zhan, C., Bai, J., Xiong, M., Li, F., Liu, Y., 2017. High-efficient sky-blue and green emissive OLEDs based on FIrpic and FIrdfpic. Synth. Met. 234, 111–116. https://doi.org/10.1016/j.synthmet.2017.10.005.

Livingston, D.C., 1954. Colorimetric analysis of the NTSC color television system. Proc. IRE 42, 138–150. https://doi.org/10.1109/JRPROC.1954.274620.

Lochner, C.M., Khan, Y., Pierre, A., Arias, A.C., 2014. All-organic optoelectronic sensor for pulse oximetry. Nat. Commun. 5, 5745. https://doi.org/10.1038/ncomms6745.

Mayr, C., Brütting, W., 2015. Control of molecular dye orientation in organic luminescent films by the glass transition temperature of the host material. Chem. Mater. 27, 2759–2762. https://doi.org/10.1021/acs.chemmater.5b00062.

Meerheim, R., Walzer, K., Pfeiffer, M., Leo, K., 2006. Ultrastable and efficient red organic light emitting diodes with doped transport layers. Appl. Phys. Lett. 89, 061111. https://doi.org/10.1063/1.2268354.

Meerheim, R., Nitsche, R., Leo, K., 2008. High-efficiency monochrome organic light emitting diodes employing enhanced microcavities. Appl. Phys. Lett. 93, 043310. https://doi.org/10.1063/1.2966784.

Mesta, M., Carvelli, M., de Vries, R.J., van Eersel, H., van der Holst, J.J.M., Schober, M., Furno, M., Lüssem, B., Leo, K., Loebl, P., Coehoorn, R., Bobbert, P.A., 2013. Molecular-scale simulation of electroluminescence in a multilayer white organic light-emitting diode. Nat. Mater. 12, 652–658. https://doi.org/10.1038/nmat3622.

Moon, C.-K., Kim, K.-H., Kim, J.-J., 2017. Unraveling the orientation of phosphors doped in organic semiconducting layers. Nat. Commun. 8791. https://doi.org/10.1038/s41467-017-00804-0.

Nakanotani, H., Masui, K., Nishide, J., Shibata, T., Adachi, C., 2013. Promising operational stability of high-efficiency organic light-emitting diodes based on thermally activated delayed fluorescence. Sci. Rep. 3,https://doi.org/10.1038/srep02127 srep02127.

Neyts, K.A., 1998. Simulation of light emission from thin-film microcavities. J. Opt. Soc. Am. A 15, 962–971. https://doi.org/10.1364/JOSAA.15.000962.

Olthof, S., Meerheim, R., Schober, M., Leo, K., 2009. Energy level alignment at the interfaces in a multilayer organic light-emitting diode structure. Phys. Rev. B. 79. 245308. https://doi.org/10.1103/PhysRevB.79.245308.

Purcell, E.M., Torrey, H.C., Pound, R.V., 1946. Resonance absorption by nuclear magnetic moments in a solid. Phys. Rev. 69, 37–38. https://doi.org/10.1103/PhysRev.69.37.

Reineke, S., Baldo, M.A., 2012. Recent progress in the understanding of exciton dynamics within phosphorescent OLEDs. Phys. Stat. Sol. A 209, 2341–2353. https://doi.org/10.1002/pssa.201228292.

Reineke, S., Baldo, M.A., 2014. Room temperature triplet state spectroscopy of organic semiconductors. Sci. Rep. 4. https://doi.org/10.1038/srep03797.

Reineke, S., Walzer, K., Leo, K., 2007. Triplet-exciton quenching in organic phosphorescent light-emitting diodes with Ir-based emitters. Phys. Rev. B. 75125328. https://doi.org/10.1103/PhysRevB.75.125328.

Reineke, S., Lindner, F., Schwartz, G., Seidler, N., Walzer, K., Lüssem, B., Leo, K., 2009. White organic light-emitting diodes with fluorescent tube efficiency. Nature 459, 234–238. https://doi.org/10.1038/nature08003.

Reineke, S., Rosenow, T.C., Lüssem, B., Leo, K., 2010. Improved high-brightness efficiency of phosphorescent organic LEDs comprising emitter molecules with small permanent dipole moments. Adv. Mater. 22, 3189–3193. https://doi.org/10.1002/adma.201000529.

Reineke, S., Thomschke, M., Lüssem, B., Leo, K., 2013. White organic light-emitting diodes: status and perspective. Rev. Mod. Phys. 85, 1245–1293. https://doi.org/10.1103/RevModPhys.85.1245.

Reymond, J.-L., Blum, L.C., van Deursen, R., 2011. Exploring the chemical space of known and unknown organic small molecules at www.gdb.unibe.ch. CHIMIA Int. J. Chem. 65, 863–867. https://doi.org/10.2533/chimia.2011.863.

Rosenow, T.C., Furno, M., Reineke, S., Olthof, S., Lüssem, B., Leo, K., 2010. Highly efficient white organic light-emitting diodes based on fluorescent blue emitters. J. Appl. Phys. 108, 113113. https://doi.org/10.1063/1.3516481.

Samuel, I.D.W., Kulyk, O., McNeill, A., Moseley, H., Ferguson, J., Ibbotson, S., 2015. Ambulatory photodynamic therapy of skin cancer. Photodiagnosis Photodyn. Ther. 12, 331. https://doi.org/10.1016/j.pdpdt.2015.07.029.

Schober, M., Olthof, S., Furno, M., Lüssem, B., Leo, K., 2010. Single carrier devices with electrical doped layers for the characterization of charge-carrier transport in organic thin-films. Appl. Phys. Lett. 97, 013303. https://doi.org/10.1063/1.3460528.

Scholz, S., Kondakov, D., Lüssem, B., Leo, K., 2015. Degradation mechanisms and reactions in organic light-emitting devices. Chem. Rev. 115, 8449–8503. https://doi.org/10.1021/cr400704v.

Segal, M., Baldo, M.A., Holmes, R.J., Forrest, S.R., Soos, Z.G., 2003. Excitonic singlet-triplet ratios in molecular and polymeric organic materials. Phys. Rev. B. 68075211. https://doi.org/10.1103/PhysRevB.68.075211.

Soneira, R.M., 2018. Galaxy S9 OLED Display Technology Shoot-Out [WWW Document]. http://www.displaymate.com/Galaxy_S9_ShootOut_1s.htm. (Accessed 26 May 2018).

Spindler, J., Kondakova, M., Boroson, M., Büchel, M., Eser, J., Knipping, J., 2018. Advances in high efficacy and flexible OLED lighting. SID 2018 DIGEST 84-1, 1135–1138.

Springer, R., Kang, B.Y., Lampande, R., Ahn, D.H., Lenk, S., Reineke, S., Kwon, J.H., 2016. Cool white light-emitting three stack OLED structures for AMOLED display applications. Opt. Express 24, 28131–28142. https://doi.org/10.1364/OE.24.028131.

Steude, A., Witts, E.C., Miles, G.B., Gather, M.C., 2016. Arrays of microscopic organic LEDs for high-resolution optogenetics. Sci. Adv. 2, e1600061. https://doi.org/10.1126/sciadv.1600061.

Su, S.-J., Gonmori, E., Sasabe, H., Kido, J., 2008. Highly efficient organic blue-and white-light-emitting devices having a carrier- and exciton-confining structure for reduced efficiency roll-off. Adv. Mater. 20, 4189–4194. https://doi.org/10.1002/adma.200801375.

Tanaka, D., Sasabe, H., Li, Y.-J., Su, S.-J., Takeda, T., Kido, J., 2007. Ultra high efficiency green organic light-emitting devices. Jpn. J. Appl. Phys. 46L10. https://doi.org/10.1143/JJAP.46.L10.

Tang, C.W., VanSlyke, S.A., 1987. Organic electroluminescent diodes. Appl. Phys. Lett. 51, 913–915. https://doi.org/10.1063/1.98799.

Thompson, M., 2007. The evolution of organometallic complexes in organic light-emitting devices. MRS Bull. 32, 694–701. https://doi.org/10.1557/mrs2007.144.

Thomschke, M., Reineke, S., Lüssem, B., Leo, K., 2012. Highly efficient white top-emitting organic light-emitting diodes comprising laminated microlens films. Nano Lett. 12, 424–428. https://doi.org/10.1021/nl203743p.

Tu, G., Zhou, Q., Cheng, Y., Wang, L., Ma, D., Jing, X., Wang, F., 2004. White electroluminescence from polyfluorene chemically doped with 1,8-napthalimide moieties. Appl. Phys. Lett. 85, 2172–2174. https://doi.org/10.1063/1.1793356.

Turro, N.J., Ramamurthy, V., Scaiano, J.C., 2010. Modern Molecular Photochemistry of Organic Molecules. University Science Books, Sausalito.

Uoyama, H., Goushi, K., Shizu, K., Nomura, H., Adachi, C., 2012. Highly efficient organic light-emitting diodes from delayed fluorescence. Nature 492, 234–238. https://doi.org/10.1038/nature11687.

Walzer, K., Maennig, B., Pfeiffer, M., Leo, K., 2007. Highly efficient organic devices based on electrically doped transport layers. Chem. Rev. 107, 1233–1271. https://doi.org/10.1021/cr050156n.

Watanabe, T., Yamaoka, R., Ohsawa, N., Tomida, A., Seo, S., Yamazaki, S., 2018. Extremely high-efficient OLED achieving external quantum efficiency over 40% by carrier injection layer with super-low refractive index. SID 2018 DIGEST 26-2, 332–335.

White, M.S., Kaltenbrunner, M., Głowacki, E.D., Gutnichenko, K., Kettlgruber, G., Graz, I., Aazou, S., Ulbricht, C., Egbe, D.A.M., Miron, M.C., Major, Z., Scharber, M.C., Sekitani, T., Someya, T., Bauer, S., Sariciftci, N.S., 2013. Ultrathin, highly flexible and stretchable PLEDs. Nat. Photon 7, 811–816. https://doi.org/10.1038/nphoton.2013.188.

Wong, M.Y., Zysman-Colman, E., 2017. Purely organic thermally activated delayed fluorescence materials for organic light-emitting diodes. Adv. Mater. 29. https://doi.org/10.1002/adma.201605444.

Wu, J.-H., Chi, C.-A., Chiang, C.-L., Chen, G.-Y., Lin, Y.-P., Chen, C.-C., Ho, S.-Y., Chen, S.-P., Li, J.-Y., 2016. Dimmable sunlight-like organic light emitting diodes with ultra-high color rendering index. Opt. Mater. 55, 90–93. https://doi.org/10.1016/j.optmat.2016.03.027.

Würfel, P., 2005. Physics of Solar Cells: From Principles to New Concepts. WILEY-VCH Verlag GmbH & Co. KGaA, Weinheim.

Yersin, H., 2004. Triplet emitters for OLED applications. Mechanisms of exciton trapping and control of emission properties. In: Transition Metal and Rare Earth Compounds, Topics in Current Chemistry. Springer, Berlin, Heidelberg, pp. 1–26. https://doi.org/10.1007/b96858.

Yokoyama, D., Sakaguchi, A., Suzuki, M., Adachi, C., 2008. Horizontal molecular orientation in vacuum-deposited organic amorphous films of hole and electron transport materials. Appl. Phys. Lett. 93, 173302. https://doi.org/10.1063/1.2996258.

Yokoyama, D., Setoguchi, Y., Sakaguchi, A., Suzuki, M., Adachi, C., 2010. Orientation control of linear-shaped molecules in vacuum-deposited organic amorphous films and its effect on carrier mobilities. Adv. Funct. Mater. 20, 386–391. https://doi.org/10.1002/adfm.200901684.

Zhang, Y., Lee, J., Forrest, S.R., 2014. Tenfold increase in the lifetime of blue phosphorescent organic light-emitting diodes. Nat. Commun. 5. https://doi.org/10.1038/ncomms6008.